JOURNAL OF CATALYSIS 100, 167–175 (1986)

X-Ray Photoemission Study of Oxygen and Nitric Oxide Adsorption on MoS_2

ZHUANG SHUXIAN,[1] W. KEITH HALL,[2] GERHARD ERTL, AND HELMUT KNÖZINGER[3]

Institut für Physikalische Chemie, Universität München, Sophienstrasse 11, 8000 Munich 2, West Germany

Received October 10, 1985; revised February 14, 1986

The adsorption of O_2 and NO on polycrystalline MoS_2 has been studied by XPS at temperatures from 80 to 300 and to 700 K, respectively. The data suggest that oxygen is adsorbed in a molecular form at low temperature on coordinatively unsaturated (cus) Mo sites in a lowered valence state and that much of it can be desorbed without oxidation of the MoS_2 as the temperature is raised to 300 K. By contrast, NO was partially dissociated at $T > 130$ K and surface oxidation became detectable at $T > 200$ K. In this respect the present results differ significantly from literature reports for reduced and/or sulfided molybdena–alumina catalysts where molecular NO adsorbs in the form of dimer or dinitrosyl species. A physisorbed state was also detected at $T \leq 180$ K. © 1986 Academic Press, Inc.

1. INTRODUCTION

Sulfided molybdena–alumina belongs to an industrially important class of heterogeneous catalysts. Thus, unsupported polycrystalline MoS_2 has frequently been studied as a model catalyst in fundamental research. Attempts have been made to elucidate the structural and electronic nature of polycrystalline MoS_2 as related to the catalytic properties of these highly disordered materials. X-Ray scattering (*1–3*), X-ray absorption (*4*), X ray (*3, 4*), UV photoemission (*5*), EXAFS (*6*), and perturbed angular correlation (TDPAC) (*7*) studies have been reported. Studies on MoS_2 single crystals have also been performed. Ion scattering experiments were directed toward elucidating surface composition and structure of the (0001) basal plane of MoS_2 (*8–10*). This basal plane is known to be chemically relatively inert unless defects are induced in the surface (*11, 12*). In fact, recent LEED, Auger, and TDS investigations by Salmeron *et al.* (*13*) and by Farias *et al.* (*15*) have shown that only weak physisorption occurs on the (0001) basal plane of MoS_2 for a variety of gases including thiophene and O_2. It is, however, well known that MoS_2 edge areas provide significant chemical reactivity (*14–19*). In an X-ray photoemission study, Suzuki *et al.* (*20*) convincingly demonstrated that NO exposure of a MoS_2 single crystal at temperatures above 570 K led to substantial oxidation in the edge areas while the basal planes remained unreactive.

Catalytically active sites are also believed to develop along the edges of MoS_2 crystals (*12, 14, 17, 18, 21*) and it has become an interesting and important task for catalytic chemists to characterize and estimate the number of these edge sites, which probably must be identified with low-valent, coordinatively unsaturated (cus) Mo^{x+} centers. Probe molecules, namely O_2 and NO, have been used for this purpose. Both low temperature O_2 adsorption and NO adsorption have been shown to successfully correlate with catalytic activity of unsupported polycrystalline MoS_2 (*14, 22, 23*) and of supported sulfided Mo-based cata-

---

[1] Permanent address: Department of Chemistry, University of Science and Technology of China, Hefei, Anhui, People's Republic of China.

[2] Permanent address: Department of Chemistry, University of Pittsburgh, Pittsburgh, Pa. 15260.

[3] To whom all correspondence should be addressed.

0021-9517/86 $3.00

lysts (*23–27*). Although the UPS results of Liang *et al.* (*5*) suggest molecular adsorption of O_2 on polycrystalline MoS_2, Abdo *et al.* (*26*) have detected that O_2^- species on reduced Mo/Al_2O_3 catalysts decompose to O^- at room temperature. Moreover, later work (*30*) has shown an approximate 4 to 1 ratio of the chemisorptions of NO (as dimeric species) to O_2 for the same sites. These data strongly suggest that oxygen is largely dissociated below room temperature. However, the result obtained may depend on many factors including pretreatment, extent of reduction or sulfiding, catalyst composition, and so on. Thus, variations may be expected since the nature of the adsorbed oxygen species and their stability on these materials have not yet been fully explored.

NO is increasingly being used by several research groups as a probe molecule, particularly because the NO chemisorption system can easily be studied by infrared transmission spectroscopy when supported catalysts are to be characterized (*27–31*). Sometimes there have been indications of chemical transformations of NO on these surfaces even at room temperature. Oxidation by NO can always be accomplished below 573 K. Interestingly, the characteristic infrared frequencies observed for the dinitrosyl or dimeric species are very nearly the same for sulfided and for reduced, sulfur-free catalysts (*30, 31*), although CO adsorption on these same materials shows that the dominant valence states in the cus Mo^{x+} sites may be different in these two differently pretreated catalysts (*31*).

In the present work we have obtained X-ray photoemission spectra of O_2 and NO adsorbed on polycrystalline MoS_2 over a wide range of temperature. A few experiments have also been carried out on a MoS_2 single crystal, and with H_2O and pyridine adsorbates for comparison.

2. EXPERIMENTAL

Photoelectron spectrometer. The experiments were made with a modified commercial XPS apparatus (Vacuum Generators, ESCA III); the experimental setup was described in detail earlier (*32*). The spectrometer chamber was equipped with a hemispherical energy analyzer and an AlK_α X-ray source ($h\nu$ = 1486.6 eV). The X-ray source was operated with a stabilized electron current of 20 mA at an acceleration voltage of 11 kV. Pretreatments of and chemisorption on the samples could be performed within a preparation chamber while the spectrometer chamber was held under UHV conditions. The base pressure was in the range 10^{-9} to 10^{-10} Torr (133.3 Torr = 1 N m^{-2}). Sample temperatures were measured with a Chromel–Alumel thermocouple. Binding energies E_b were referenced to the C 1*s* signal at 284.6 eV, the accuracy of the E_b values being ±0.1 eV. Significant charging effects were not observed with the MoS_2 samples, which were pressed into a 0.7-cm-wide and 0.05-cm-deep cavity in a stainless-steel sample holder. The single crystal was mounted onto the sample holder by means of tungsten wires.

When required, relative surface concentrations C_x were determined by

$$C_x = \frac{A_x}{q_x}\left[\sum_{i=1}^{n}\frac{A_i}{q_i}\right]^{-1} \quad (1)$$

from the XPS peak areas A_i, where the q_i are experimental photoionization cross sections as given by Wagner (*33*) for the various elements present in the surface.

Adsorbates. O_2 and NO were high-purity Linde products. NO was distilled between traps which were cooled to dry ice and liquid N_2 temperatures, respectively. O_2 was passed through a trap at liquid N_2 temperature. Freshly distilled H_2O and pyridine were degassed by a series of freeze pump–thaw cycles prior to adsorption experiments.

Molybdenum disulfide. The MoS_2 single crystal was kindly made available by Professor A. Wold.

The polycrystalline MoS_2 was prepared from $(NH_4)_2MoS_4$ by thermal decomposi-

TABLE 1

X-Ray Photoemission Data for Polycrystalline MoS_2

Sample treatment	Binding energy E_b (eV)					C_x (%)				[S]/[Mo]
	Mo $3d_{5/2}$	Mo $3d_{3/2}$	S $2p$	O $1s$	C $1s$	Mo	S	O	C	
Without H_2 treatment	229.1	232.2	162.0	532.0	284.6	17.1	38.4	9.5	35.0	2.2
After H_2 treatment[a]	229.0	232.1	162.0	~532	284.6	24.2	53.7	5.4	16.8	2.2

[a] Repeated treatments, 50–100 Torr H_2 at 720 K for 1–2 h.

tion and reductive treatment in H_2/H_2S (9/1) at 620 K for 2h. The N_2 BET surface area of the resulting MoS_2 was approximately 60 $m^2\ g^{-1}$. After this material was mounted onto the manipulator head in air and transferred into the spectrometer, it was contaminated by carbon and oxygen as indicated by the initial spectrum. Repeated reductions in 50–100 Torr H_2 at 720 K for 1–2 h in the preparation chamber reduced these contaminations significantly (see Table 1); besides the C 1*s* peak at 284.6 eV and on O 1*s* peak at 532.0 eV no other impurities were detected. The Mo 3*d* and S 2*p* peaks are found at the positions and intensity ratios characteristic of MoS_2 (*34*) with no detectable indication of Mo oxidation states other than Mo^{4+} or of any sulfur species other than sulfide (see Fig. 1). The [S]/[Mo] ratio as estimated according to Eq. (1) turned out to be 2.2 after *in situ* H_2 treatment and is close to the stoichiometric value for MoS_2. The accuracy of this estimate is certainly far too low to deduce any reliable indication of nonstoichiometry.

Gas adsorption. The H_2-treated samples were evacuated to about 5×10^{-9} Torr in the preparation chamber. In order to reduce the contamination of the sample by residual gases, the sample was transferred into the spectrometer chamber (base pressure 5×10^{-10} Torr) prior to cooling. When a temperature of 80 K was reached, the sample was transported back into the preparation chamber, and gas exposure was carried out there at various pressures, followed by evacuation to below 10^{-7} Torr. The pumping time was typically from sev-

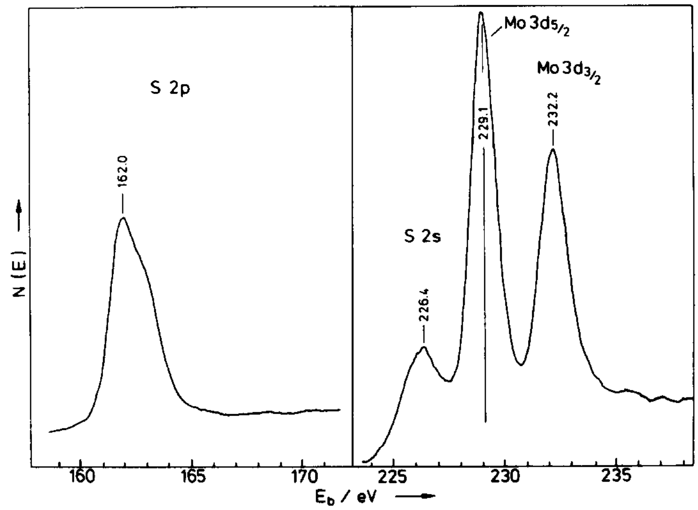

FIG. 1. X-Ray photoelectron spectra of polycrystalline MoS_2 (S 2*p* and Mo 3*d* region) after H_2 treatment (200 Torr, 2 h, 873 K).

eral minutes up to 30 min, depending on the gas treatment. The sample was then transferred into the spectrometer chamber for XPS studies, the base pressure being typically in the range 10^{-8} Torr. Desorption occurred on raising the sample temperature and associated spectral changes could be followed accordingly.

3. RESULTS

Oxygen adsorption. Figure 2 shows O 1*s* spectra obtained after exposure of polycrystalline MoS_2 to O_2 at 80 K. A broad peak developed the intensity of which increased with exposure. The position of this peak was independent of exposure with a binding energy of 533.2 eV. The peak intensity was drastically reduced during desorption by increasing the sample temperature (Fig. 2) and at 150 K only about 20% of the initial oxygen coverage was retained. The binding energy began to shift to lower values at $T > 130$ K and after desorption at 300 K only a weak broad feature at 532.0 eV was observed. The characteristic photoemission data for O_2 adsorption on MoS_2 are summarized in Table 2. Identical spectra with correspondingly lower intensities were observed for O_2 adsorbed on the MoS_2 single crystal. Other changes in the XPS spectra were not detected (in either the S 2*p* or the Mo 3*d* region). This shows that detectable surface oxidation of the MoS_2 had not occurred, confirming the observations of Davis and Carver (*35*).

TABLE 2

Characteristic Photoelectron Data for O_2 Adsorption on Polycrystalline MoS_2[a]

T (K)	E_b(O 1*s*) (eV)	[Py]/[Mo][b]	[O_2]/[Mo]
80	533.2	—	0.20
300	532.0	—	0.02
80	533.3	0.05	0.13

[a] For exposures see legends to Figs. 2 and 4.

[b] Pyridine preadsorbed at 230 K.

As the observed O 1*s* binding energies were close to the regime in which condensed or physisorbed water would give rise to photoemission, the effect of H_2O adsorption was tested. H_2O was exposed to polycrystalline MoS_2 at 80 K and desorbed at temperatures in the range $80 \leq T \leq 300$ K. The O 1*s* emission from condensed H_2O in fact appeared at 533.7 eV, close to the E_b value of 533.2 eV observed for adsorbed oxygen. The desorption behavior of adsorbed H_2O and O_2, however, differed greatly. As shown in Fig. 3, the intensity of the peak at 533.7 eV due to adsorbed water remained almost constant at temperatures $T < 170$ K and then dropped steeply to a very low intensity peak as water was removed. The final weak feature had a binding energy of 532.7 eV, presumably due to hydroxyl groups (*36*). By contrast, the intensity of the peak at 533.2 eV due to ad-

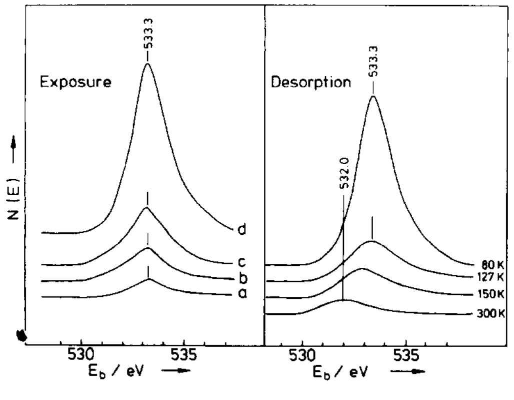

FIG. 2. O 1*s* spectra (background subtracted) of oxygen adsorbed on polycrystalline MoS_2 recorded after exposure at 80 K: (a) 100 L, (b) 150 L, (c) 1×10^{-5} Torr for 5 min, (d) 1 Torr for 10 min, and after desorption at increasing temperatures. (1 L = 10^{-6} Torr · s.)

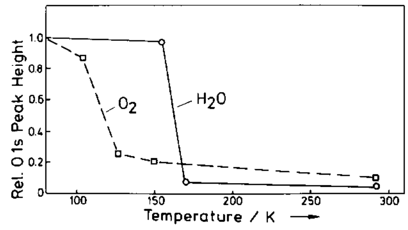

FIG. 3. Desorption behavior of O_2 and H_2O from polycrystalline MoS_2. (For typical O_2 adsorption conditions see Fig. 2; H_2O adsorption at 4 L and 80 K prior to desorption under continuous evacuation.)

sorbed oxygen immediately decreased while the sample was warmed above 80 K; the O 1*s* peak intensity decreased to only 20% of its initial value after desorption at 150 K, a temperature at which the O 1*s* signal due to water adsorption had not changed at all. It is therefore evident that the photoemission observed at 533.2 eV after O_2 exposure must be due to adsorbed oxygen and cannot be produced by any uncontrolled adsorption of water from background gas in the chamber.

As oxygen adsorption is expected to occur on cus Mo^{x+} sites which should exhibit Lewis acidity, some experiments were performed to test the effect of preadsorption of a Lewis base, namely pyridine, on the adsorption of O_2. When pyridine was adsorbed on MoS_2 at 80 K, C 1*s* and N 1*s* photoemission peaks developed at 286.0 and 400.1 eV, respectively; these could be assigned to condensed pyridine (*37*). After desorption at 300 K, these peaks were strongly reduced in intensity and shifted to 285.6 and 399.7 eV. The corresponding pyridine species is presumed to be coordinated to cus Mo^{x+} sites. O_2 adsorption was carried out on a MoS_2 sample at 80 K after 900 L exposure of pyridine at 80 K and desorption at 230 K. The resulting C 1*s* and N 1*s* peaks are shown in Fig. 4. The [pyridine]/[Mo] ratio as estimated from the peak intensities of the C 1*s* and Mo 3*d* emissions was 0.05. The O 1*s* peaks after O_2 adsorption (1.4 Torr for 5 min) at 80 K are also shown in Fig. 4. The photoemission peak was centered at 533.3 eV, the same binding energy found without pyridine preadsorption. The O_2 coverage obtained under comparable conditions, however, was reduced by a factor of about 1.4 (see Table 2) and desorption was significantly facilitated; the amount retained after desorption at 170 K was nearly undetectable. These results suggest that indeed cus Mo^{x+} sites which develop Lewis acidity are involved in adsorption of oxygen.

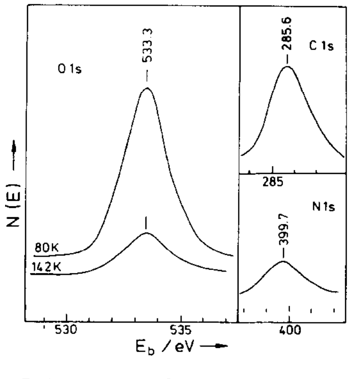

FIG. 4. O 1*s* spectra of oxygen adsorbed on polycrystalline MoS_2 precovered with pyridine; C 1*s* and N 1*s* spectra of pyridine are also shown. (Exposure to pyridine vapor at 300 L and 80 K followed by evacuation at 230 K and exposure to 1.4 Torr O_2 for 5 min at 80 K.)

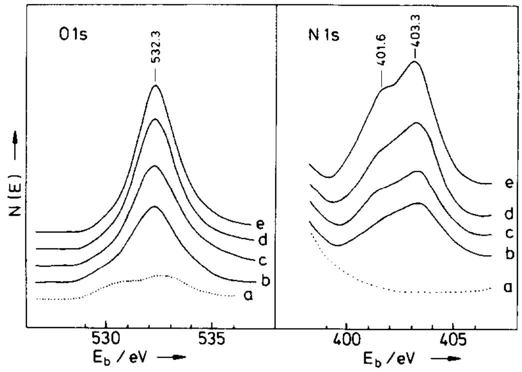

FIG. 5. O 1*s* and N 1*s* spectra of NO adsorbed on polycrystalline MoS_2 at 80 K after various exposures: (a) background, (b) 0.1 Torr for 5 min, (c) 0.1 Torr for 10 min, (d) 0.1 Torr for 20 min, (e) 0.1 Torr for 50 min.

Nitric oxide adsorption. The O 1*s* and N 1*s* spectra of NO adsorbed at 80 K on polycrystalline MoS_2 are shown in Fig. 5. The adsorption pressure was 0.1 Torr NO and the spectra are shown as they develop with exposure time. The O 1*s* spectra are dominated by a peak centered at 532.3 eV. In the N 1*s* region, a broad emission peak developed between 400 and 405 eV. At the highest exposures the N 1*s* profile clearly revealed two distinct contributions at 401.6 and 403.3 eV. The atomic ratio between nitrogen and oxygen was estimated from the N 1*s* and O 1*s* peak intensities to be 0.82.

During desorption (continuous evacuation) at increasing temperatures (see Fig.

6), the O 1*s* peak at 532.3 eV decreased and a shoulder developed at 530.3 eV at temperatures $T \geq 180$ K; this shoulder became resolved into a distinct peak on further increasing the temperature. At $T > 240$ K, two emissions were resolved at 530.3 and 532.3 eV and the former became the dominant feature after desorption at 440 K. Simultaneously, the intensity in the N 1*s* region was continuously eroded, the peak intensity at 401.6 eV decreasing significantly faster than the one at 403.3 eV as the temperature was increased. By 180 K this emission had disappeared (physisorption) while the other two remained distinguishable up to 293 K. These two photoemission peaks are evidently due to two inequivalent adsorbed NO species. A third N 1*s* photoemission peak at 400.3 eV became detectable at 180 K, and its intensity first increased with temperature up to 195 K and then decreased again. At 293 K only a weak emission remained. After desorption at 440 K the N 1*s* photoemission had completely disappeared.

When the MoS_2 sample was exposed to NO at elevated temperature, evidence for surface oxidation was obtained. As shown in Fig. 7, on exposure to 0.01 Torr NO for 15 min at 700 K, a strong O 1*s* peak at 530.3 eV appeared while no photoemission could be detected in the N 1*s* region. The [O]/[Mo] atomic ratio was estimated to be 0.9 after this treatment. (O 1*s* binding energies of 531.1 and 530.8 eV have been reported (*34*) for MoO_3 and MoO_2, respectively.)

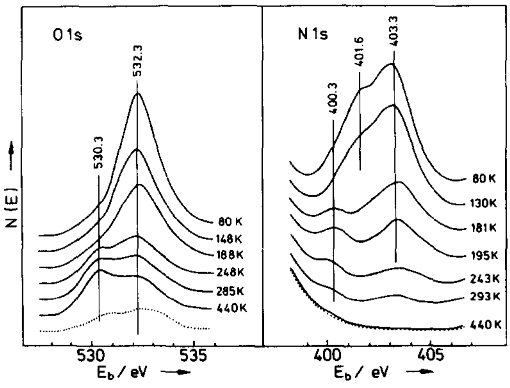

FIG. 6. O 1*s* and N 1*s* spectra after NO desorption (continuous evacuation) from polycrystalline MoS_2 at the temperatures indicated (dotted line indicates background prior to adsorption).

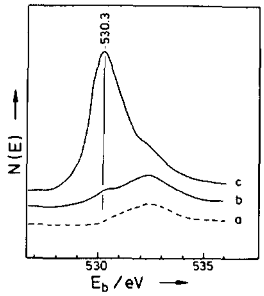

FIG. 7. O 1*s* spectra after surface oxidation of polycrystalline MoS_2 by NO exposure at elevated temperatures: (a) background, (b) 300 L NO at 300 K, (c) 0.01 Torr NO for 15 min at 700 K.

4. DISCUSSION

As summarized in Table 2, O_2 adsorption at 80 K on MoS_2 yielded a photoemission peak at 533.2 eV which corresponded approximately to an $[O_2]/[Mo]$ ratio of 0.2. It may be assumed that this is a molecular form of oxygen; the peak at 532.0 eV which appears at higher temperatures may be assumed to stem from a dissociated form bonded to the surface; it is also observed as the contamination which could not be completely removed with H_2. The pyridine preadsorption experiments suggested that cus Mo^{x+} sites are involved in oxygen adsorption. It is interesting to note in this context that sulfur chemisorption near monolayer coverage on a Mo(100) surface essentially blocked oxygen adsorption (*15*).

O_2 adsorption on metal surfaces at low temperatures where dissociative chemisorption appears to be unlikely gave rise to photoemission peaks in the range of binding energies between 532 and 534 eV (*38*). The fact that the peak at 533.2 eV was not due to H_2O contamination supports the assignment of this photoemission to adsorbed dioxygen, and we suggest that oxygen adsorption is molecular at 80 K when used for surface titration via O_2 uptake on unsupported MoS_2 (and presumably on supported sulfided catalysts). The UPS results reported by Liang *et al.* (*5*) for oxygen adsorption on poorly crystallized MoS_2 is in agreement with this assignment. Abdo *et al.* (*26*), when studying oxygen adsorption on sulfided Mo/Al_2O_3 catalysts at 93 K by electron spin resonance, observed the characteristic signal of O_2^- species in amounts considerably less than the total adsorption. In this same study, O^- species were detected when the temperature was raised to room temperature. The photoemission peak observed at 532.0 eV after desorption at 300 K (see Table 2) may thus be assigned to an atomic species. This is substantiated by the work of Valyon and Hall (*30*), who found a ratio of 4 : 1 for dinitrosyl NO and O_2 chemisorption shown to occupy the same sites.

Table 3 summarizes N 1*s* and O 1*s* binding energies which were reported for NO adsorption on metallic Ni (*39*) and on the Ag(111) face (*40*). As can be seen, E_b values for both N 1*s* and O 1*s* levels vary over a wide range and a variety of different chemisorption species have been identified on the basis of these E_b values.

NO adsorption at 80 K on MoS_2 produced on O 1*s* peak at E_b = 532.3 eV and two signals in the N 1*s* region, namely at 401.6 and 403.3 eV (see Fig. 5). These two photoemission peaks indicate the presence of two distinct NO species, although these are not characterized by different O 1*s* peaks. The species connected with the peak at 401.6 eV desorbs at temperatures below 180 K and thus may be supposed to be physisorbed NO. The second species (E_b = 403.3 eV) is still detected at 293 K. Infrared studies of NO adsorption at room temperature on sulfided Mo/Al_2O_3 catalysts (*27–31*) have provided convincing evidence for the formation of NO dimers or dinitrosyl species. We therefore may assign the N 1*s* photoemission at 403.3 eV to this species.

The third N 1*s* emission peak at 400.3 eV, which first became noticeable at 180 K in Fig. 6 and the intensity of which appears to pass through a maximum near 200 K, is in a binding energy region attributable to atomic nitrogen. The appearance of this photoemission peak may thus indicate that NO dissociation has occurred at temperatures higher than approximately 130 K. This assignment is supported by the temperature dependence of the peak intensity. The in-

TABLE 3

N 1*s* and O 1*s* Binding Energies of Adsorbed NO

Adsorbent	*T* (K)	Binding energy (eV)		Assignment	Ref.
		N 1*s*	O 1*s*		
Ni	80	397.5	529.5	Atomic N and O	(*39*)
		399.5	530.7	Bent NO	(*39*)
		402		Linear NO	(*39*)
		405.5		Physisorbed	(*39*)
Ag(111)	25	399.6	530.9	Bridging NO	(*40*)
		401.9	534.6	Physisorbed	(*40*)
		405.2	537.9		
MoS_2	80	401.6	532.3	Physisorbed	This work
		403.3		Dimer	
	248	400.3	530.3	Dissociative	
		403.3	532.3	Dimer	
	440	—	530.3		
	700	—	530.3		

crease with temperature below 200 K would result from increased NO dissociation; the decrease at higher temperatures would then be expected due to atom recombination and desorption of dinitrogen. Thus, atomic oxygen would be retained on the surface and lead to surface oxidation as evidenced by the buildup of a photoemission peak at 530.3 eV at temperatures above 200 K.

The oxidation of MoS_2 by NO at elevated temperature is clearly demonstrated by the spectra of Fig. 7. These results are in excellent agreement with data reported by Suzuki *et al.* (*20*), who observed an O 1*s* emission at 530.5 eV when the edge area of a MoS_2 single crystal was oxidized by NO at 570 K. These authors also identified the appearance of a small Mo^{6+} contribution in the Mo 3*d* region and they detected the evolution of SO_2 and N_2 during NO exposure.

5. CONCLUSIONS

(a) The X-ray photoemission data presented above suggest that oxygen is adsorbed in a molecular form at low temperatures on MoS_2. Although oxygen dissociation may occur as the temperature is raised to 300 K, this surprisingly does not seem to lead to any *detectable* molybdenum oxidation since the Mo 3*d* spectra remained unchanged.

(b) By contrast, the data suggested that NO reacts at comparably low temperatures and leads to (surface) oxidation at temperatures significantly below 300 K. That NO is apparently a better oxidizing agent than O_2 is remarkable and indeed seems to contradict experience with some infrared transmission studies carried out on supported catalysts at room temperature. Thus, conceivably, reported infrared spectra of NO adsorbed on supported Mo catalysts in the sulfided state may not reflect the nature of coordination sites on fully sulfided catalysts, but rather may be characteristic of a partially reoxidized material. Further work is needed to clarify the questions raised by the present work.

ACKNOWLEDGMENTS

This research was financially supported by the Deutsche Forschungsgemeinschaft. The work was initiated during a research stay in Munich of W.K.H. as a Humboldt Awardee. Z.S. received a grant from the Hans Seidel-Stiftung. We are also grateful to Professor Aaron Wold of Brown University, Providence, Rhode Island, for making available to us several single crystals of MoS_2 and to the National Science Foundation for support of related work in the United States under Grant CHE-85-12520.

REFERENCES

1. Chien, F. Z., Moss, S. C., Liang, K. S., and Chianelli, R. R., *J. Phys. Colloq.* (*France*) **42,** 273 (1981).
2. Liang, K. S., de Neufville, J. P., Jacobson, A. J., Chianelli, R. R., and Betts, F., *J. Non-Cryst. Solids* **35/36,** 1249 (1980).
3. Liang, K. S., Cramer, S. P., Johnston, D. C., Chang, C. H., Jacobson, A. J., de Neufville, J. P., and Chianelli, R. R., *J. Non-Cryst. Solids* **42,** 345 (1980).
4. Cramer, S. P., Liang, K. S., Jacobson, A. J., Chuang, C. H., and Chianelli, R. R., *Inorg. Chem.* **23,** 1215 (1984).
5. Liang, K. S., Hughes, G. J., and Chianelli, R. R., *J. Vac. Sci. Technol. A* **2,** 991 (1984).
6. Huntley, D. R., Parham, T. J., Merrill, R. P., and Sienko, M. J., *Inorg. Chem.* **22,** 4144 (1983).
7. Butz, T., Vogdt, C., Lerf, A., and Knözinger, H., *Polyhedron* **5,** 95 (1986).
8. Davis, S. M., Carver, J. C., and Wold, A., *Surf. Sci.* **124,** L12 (1983).
9. Beuken, J.-M. and Bertrand, P., Paper presented at 7th European Conference on Surface Science (ECOSS 7), Aix-en-Provence, April 1985. *Surf. Sci.*, in press.
10. Margraf, R., Taglauer, E., and Knözinger, H., unpublished results.
11. Williams, R. H., and McEvoy, A. J., *J. Phys. D* **4,** 456 (1971).
12. Ratnasamy, P., and Sivasanker, S., *Catal. Rev.-Sci. Eng.* **22,** 401 (1980).
13. Salmeron, M., Somorjai, G. A., Wold, A., Chianelli, R. R., and Liang, K. S., *Chem. Phys. Lett.* **90,** 105 (1982).
14. Hall, W. K., *in* "The Chemistry and Physics of Solid Surfaces" (R. Vanselow and R. Howe, Eds.), Vol. VI. Springer-Verlag, New York, 1986; and earlier references quoted therein.
15. Farias, M. H., Gellman, A. J., Somorjai, G. A., Chianelli, R. R., and Liang, K. S., *Surf. Sci.* **140,** 181 (1984).
16. Stevens, G. C., and Edmonds, T., *J. Less-Common Met.* **54,** 321 (1977).
17. Tanaka, K., and Okuhara, T., *Catal. Rev.-Sci. Eng.* **15,** 249 (1977).

18. Tanaka, K., and Okuhara, T., *J. Catal.* **78,** 155 (1982).

19. Chianelli, R. R., Ruppert, A. F., Behal, S. K., Kear, B. H., Wold, A., and Kershaw, R., *J. Catal.* **92,** 56 (1985).

20. Suzuki, K., Soma, M., Onishi, T., and Tamaru, K., *J. Electron Spectrosc. Relat. Phenom.* **24,** 283 (1981).

21. Topsøe, H., Clausen, B. S., Candia, R., Wivel, C., and Mørup, S., *Bull. Soc. Chim. Belg.* **90,** 1189 (1981).

22. Tauster, S. J., Pecoraro, T. A., and Chianelli, R. R., *J. Catal.* **63,** 515 (1980).

23. Bodrero, T. A., and Bartholomew, C. H., *J. Catal.* **84,** 145 (1983).

24. Bachelier, J., Duchet, J. C., and Cornet, D., *Bull. Soc. Chim. Belg.* **90,** 1301 (1981).

25. Millman, W. S., and Hall, W. K., *J. Catal.* **59,** 311 (1979); "Proceedings, 7th Int. Congr. Catal., Tokyo, 1980," Part B, p. 1304 (1981).

26. Abdo, S., Howe, R. F., and Hall, W. K., *J. Phys. Chem.* **82,** 969 (1978).

27. Millman, W. S., and Hall, W. K., *J. Phys. Chem.* **83,** 427 (1979); *Polyhedron,* in press.

28. Peri, J. B., *J. Phys. Chem.* **86,** 1615 (1982).

29. Topsøe, N.-Y., and Topsøe, H., *J. Catal.* **75,** 354 (1982); **84,** 386 (1983).

30. Valyon, J., and Hall, W. K., *J. Catal.* **84,** 216 (1983).

31. Delgado, E., Fuentes, G. A., Hermann, C., Kunzmann, G., and Knözinger, H., *Bull. Soc. Chim. Belg.* **93,** 735 (1984).

32. Ertl, G., and Thiele, N., *Appl. Surf. Sci.* **3,** 99 (1979).

33. Wagner, C., *Anal. Chem.* **44,** 1050 (1972).

34. Patterson, T. A., Carver, J. C., Leyden, D. E., and Hercules, D. M., *J. Phys. Chem.* **80,** 1700 (1976).

35. Davis, S. M., and Carver, J. C., *Appl. Surf. Sci.* **20,** 193 (1984).

36. Fusy, J., Alnot, M., Jupille, J., Pareja, P., and Ehrhardt, J. J., *Appl. Surf. Sci.* **17,** 415 (1984).

37. Inoue, Y., Kishi, K., and Ikeda, S., *J. Electron Spectrosc. Relat. Phenom.* **31,** 109 (1983).

38. Wandelt, K., *Surf. Sci. Rep.* **2,** 1 (1982).

39. Carley, A. F., Rassias, S., Roberts, M. W., and Wang Tan-Han, *J. Catal.* **60,** 385 (1979).

40. Behm, R. J., and Brundle, C. R., *J. Vac. Sci. Technol. A* **2,** 1040 (1984).